CR-184243

EVALUATION OF HIGH REYNOLDS NUMBER FLOW IN A 180 DEGREE TURN-AROUND-DUCT

by
V. A. Sandborn and S. J. Marcy

Colorado State University
Fort Collins, Colorado

ABSTRACT

Mean and turbulent velocities were measured for the flow in a 180 degree turn-around-duct over a Reynolds number range from 600,000 to greater than 900,000. The measurements were made in water using a forward scattering laser velocimeter. A duct of 100x10 centimeters constant cross-section, with a mean radius of curvature (centerline) of 10 centimeters was employed for the study.

The measurements are in agreement with previous studies in that the use of the local bulk velocity to non-dimensionalize the mean and turbulent velocities reduce the Reynolds number variations. The basic phenomenon of relaminarization along the inner surface at the start of the turn, and flow separation along the inner surface at the exit of the turn are similar to the flow observed at low Reynolds numbers. The separation bubble region shows a systematic variation with Reynolds number, however the Reynolds number effect may be of second order in the calculation of the overall flow.

Large tangential, radial and lateral turbulent velocities are measured along the outer surface of the turn.

INTRODUCTION

The development of computer codes to predict complex shear flows require experimental data over a wide range of Reynolds numbers. The present study was a continuation of the documentation of the flow in a turn-around-duct for high Reynolds numbers. The flow in the duct at lower Reynolds was reported by Sandborn and Shin (1990).

Early attempts to compute the flow in turn-around-ducts, (see Monson, et al. (1990) for a review of the earlier work), using the k-ε models for turbulent flow, were not able to accurately predict the pressure drop through the duct. Difficulty was also encountered in predicting a separation bubble at the exit of the duct. More recent computations employing a curvature term, referred to as a turbulent Richardson number, have greatly improved the ability to predict both the pressure distribution and the separation, Cheng (1990) and Monson, et al. (1990).

The present study extends the measurements in the turn-around-duct from Reynolds numbers of 500,000 to near 1,000,000. A forward scattering, laser velocimeter was employed to measure the tangential and radial mean and turbulent velocities. Hot, film and wire anemometers were employed to determine the lateral turbulent component in the duct's curved section. Estimates of the surface shear stress along the surface of the turn were obtained using a Stanton tube.

EXPERIMENTAL STUDY

Flow Facility.- Detailed descriptions of the flow facility were given by Sandborn and Shin (1990). The duct was nominally 100x10 cm in cross-section and produced a near two-dimensional flow. Measurements of the two-dimensional character of the flow were demonstrated by Sandborn and Shin. For the present study the dimensions of the duct are slightly altered, as noted on figure 1. The lateral distance of 100 cm was maintained, but the radial spacing could not be held accurately to 10 cm once the facility was cleaned and strengthened for the high Reynolds number runs. Trip wires, 1.3 mm in diameter, were employed at the inlet of the facility for the present tests. These trip wires were also employed for some of the previous low Reynolds number flows. A 12.7 mm mesh screen was employed at the exit of the duct for the present tests. Location of all instrumentation was the same at that used in the earlier studies.

Using the 12.7 mm mesh screen, the inlet pressure in the duct is approximately 1.5 atmospheres for the highest flow rates (-1.37 cubic meters pre second, Re = 950,000). For these flow conditions very small bubbles of cavitation were observed close to the inner surface near the start of the turn. No measurements were made in the turn once cavitation occurred, although there was no evidence to suggest that the flow was affected by the cavitation. The safety limits of the duct were being approached for these high flow rates, so no attempt was made to increase the duct pressure by increasing the exit screen resistance.

Velocity, Pressure and Surface Shear Stress Evaluation.- The tangential and radial mean and turbulent velocities, as well as the Reynolds turbulent shear stress were measured with the forward scattering laser velocimeter. A 20 milliwatt He-Ne laser was employed for the light source. The doppler signals were sensed with a photodiode and evaluated with a commercial doppler frequency counter system. Details of the velocimeter, signal evaluation and uncertainties in the measurements were given by Shin (1990). For the present high flow rates the uncertainties are greater due to an increase in the facility vibrations and also difficulties in excessive water being splashed on the laser optics.

The static pressure distributions around the duct were evaluated both with diaphragm pressure transducers and with mercury and heavy oil manometers.

A "razor blade" type Stanton tube described by Shin (1990) was employed to evaluate the surface shear stress at a number of locations around the outer surface of the turn. The Stanton tube was calibrated at a location upstream of the turn where the local surface shear stress was determined by fitting the measured mean velocity profiles to the "law of the wall".

Lateral Turbulent Velocity Evaluation.- It was impossible to measure the lateral velocity component with the laser velocimeter, so single yawed hot, film and wires were employed. The sensors were placed in the flow at the same location as the sampling volume of the laser velocimeter -set to measure the tangential velocity component. The velocity obtained from the laser velocimeter was employed to calibrate the thermal anemometer. Calibration of the thermal sensor sensitivity for both velocity and angle fluctuations were obtained. It was not possible to maintain the thermal sensor calibrations for extended periods of time. The laser provides an update of the calibration at each measured point. Only the thermal sensor sensitivity to the velocity fluctuations needed to be determined for most of the measurements. The sensor sensitivity to velocity at the yaw angle (30degrees) and the sensitivity to angle are proportional to the sensitivity when the wire is normal to the flow, Sandborn (1972) (page 290). The sensors were limited in strength, so it was impossible to extend the measurements to the highest Reynolds numbers.

RESULTS

Tables I through VII list the measurements obtained during the course of the study. The measured pressure coefficients are listed in Table Ia, and extrapolated values for specific Reynolds numbers are listed in Table Ib. The measured values of the mean and turbulent properties obtained with the laser velocimeter are listed in Table II. Table III lists the extrapolated values of the mean and turbulent tangential velocities divided by the local bulk velocities for specific Reynolds numbers. Table IV lists the velocities measured in the separation bubble region, and Table V gives the extrapolated values. Table VI lists the values of surface shear obtained from the Stanton tube. Table VII lists the values of the velocities obtained during the evaluation of the lateral velocities.

Figure 2 shows the static pressure coefficient variation around the turn on both the inside and outside walls for the range of Reynolds numbers from 600,000 to 1,000,000. The effect of Reynolds number on the pressure distribution is extremely small. The pressure difference between the present results and the earlier, lower Reynolds numbers, Sandborn and Shin (1990), is also noted on figure 2. The slight difference between the present results and the earlier data may be due in part to the small change in the duct dimensions.

Figure 3 shows the mean velocity distributions obtained at several locations around the duct. The use of the local bulk velocity and duct height to nondimensionalize the profiles result in near similar distributions at each location. The lower Reynolds number results are also noted on figure 3. The deviations between the earlier data and the present measurements might have been expected from the slight change in the pressure distribution.

Only when the separation bubble appears does a measurable deviation with Reynolds number occur. Figure 4 shows the mean velocity variations measured in the separation bubble region. The previous low Reynolds number data indicated a large variation in the separation region velocities up to Re = 300,000, and a lesser variation for the higher values of Re. The present results indicate the maximum bubble thickness occurs around a Reynolds number of 600,000 and the bubble decreases slightly for greater values of Re. The increasse in separation bubble thickness with increasing Reynolds number is contrary to that observed for normal turbulent boundary layers. It would appear that the separation in the turn-around-duct is at least in part governed by the enertia effects of the turn. The flow along the inner surface proceeds for an appreciable distance in the adverse pressure gradient and only separates when it is required to turn quickly. The thicking of the separation bubble may indicate the failure of the higher speed flow to make the turn. Above a Reynolds number of 600,000 the flow responds more closely to what is expected in a viscous dominated separation.

The separation bubble region for the turn-around-duct is a highly time dependent flow. As reported by Sandborn and Shin (1990), the tangential turbulent velocities at the height of the zero velocity location may be as great as 0.6Um. At the this height the flow was reversed approximately 65 percent of the time. Even very close to the surface the flow was reversed only 80 to 85 percent of the time. It appears that the flow fluctuates in a coherent manor, since the correlation between the tangential and radial velocities is extremely large and postive. The large postive correlations require that when a postive tangential velocity occurs a corresponding postive radial velocity is present.

Figure 5 compares the present measurements in the separation region at the exit of the turn with the measurements of Monson, et al. (1989). Although, comparison of the flow in the present water duct and the air duct of Monson, et al. appear similar upstream of separation, it is apparent that the character of

the separated regions are different. The present flow separation bubble is not as large, nor is the reverse flow as great as that reported for the air duct. The water duct employs an exit screen 4.3H downstream of the turn. The measurements of Sandborn and Shin (1990) found only secondary changes in the separation for flows with and without the screen in place. The air facility contained a straight exit section of approximately 14H in length. The static pressure coefficient downstream of the turn for the air facility reaches a constant value of -0.05, while the water facility indicated values of the order of -0.03 to -0.04.

Figure 6 shows the values of surface shear stress obtained with the Stanton tube. In the turn region the affect of Re on the skin friction coefficient was very small. The data for the location 1.7H upstream of the turn is not included on figure 6, since it was employed to calibrate the Stanton tube.

It was not possible to measure the surface shear along the inner wall of the turn. Shin (1990) made estimates for the low Reynolds number flows, assuming an emperical turbulent boundary layer, skin friction equation could be employed. It is questionable whether the flow along the inner surface can be considered a turbulent boundary layer. As a first approximation for the surface shear on the inner wall at the 90 degree location, a simple laminar approximation was made, as noted on the insert of figure 6. Values of the surface shear on the inner wall would appear to be of the similar magnitude as those on the outer wall. The values of surface shear noted on the insert at 170 and 180 degrees around the turn, 5.08cm and 7cm downstream of the turn were estimated from the slope of the velocity distributions at the surface.

Figure 7 shows the tangential turbulent velocity distributions obtained for a number of locations around the duct. Only secondary effects of Reynolds number are observed at a given location. The previous low Reynolds number measurements of Sandborn and Shin indicated a more pronounced variation of the turbulent velocities with Reynolds number. Although, the low Reynolds number measurements suggested an uncoupling between the turbulent velocities and the mean flow, the higher flows indicate near similarity for both mean and turbulent quantities with Reynolds number.

Figure 8 is a plot of the tangential, u, radial, v, and lateral, w, tubulent velocity components evaluated at 50, 90, and 130 degrees around the turn. Measurements with the hot wires and films proved very difficult in the high Reynolds number flow regime. It was impossible to maintain the calibration of either wires or films for any apprecable length of run time. The film sensors failed before a profile could be completed. Althought the accuracy of the lateral turbulent velocities was poor, it appears that the peak magnitude of the lateral and radial velocities are roughly equal in the outer part of the shear layer along the outer wall. Very close to the outer wall the lateral velocity component was larger than either of the other two velocity components. It appears incorrect to employ the approximation that the lateral component is the average of the tangential and radial components, as is the case for normal turbulent boundary layers. The large values of both the lateral, w', and radial, v', velocities would be consistent with the presence of a vortex type motion along the outer wall in the turn. At the 50 degree location around the turn, which is just downstream of the apparent start of the large disturbances, all three components of the turbulence are found to be of the same magnitude. Further around the turn the radial and lateral components remain large, while the tangential velocity fluctuations are reduced in intensity.

CONCLUSIONS

The mean and turbulent velocities in a 180 degree, turn-around-duct for a Reynolds number range from 600,000 to greater than 900,000 have been documented. Tabulated values are given for the static pressure, mean and turbulent velocities, and surface shear stress on the outer surface.

The effects of Reynolds number are reduced by employing the local bulk velocity and duct height as the characteristic velocity and length. Systematic variation with Reynolds number of the flow field in the separation bubble, which occured along the inner surface at the exit of the turn, was documented in detail.

REFERENCES

Cheng, G. C. (1990) Numerical Compulations and Turbulent Modeling of Turbulent Flows with Streamline Curvature. PhD Dissertation, University of Kansas.

Monson, D.J., Seegmiller, H.L., McConnaughey, P.K. and Chen, Y.S. (1990) Comparison of Experiment with Calculations Using Models for a Two-Dimensional U-Duct. AIAA paper No. 90-1484, given at 21st Fluid Dynamics and Laser Conference, Seattle, WA, June 18-20, 1990.

Sandborn, V.A. and Shin, J.C. (1990) Water Flow Measurements in a 180 Degree Turn-Around Duct. Final report NASA Contract No. NAS8-36354.

Shin, J.C. (1990) Experiments on Turbulent Shear Flow in a Turn-Around Duct. PhD Dissertation, Colorado State University.

LIST OF SYMBOLS

c_f	Skin friction coefficient, $\tau_w/\frac{1}{2}\rho U_m^2$
c_p	Static pressure coefficient, $\Delta p/\frac{1}{2}\rho U_m^2$
H	Duct height
p	Local static pressure
Re	Reynolds number
T	Water Temperature
u′	Root-mean-square of the tangential turbulent velocity
U	Local mean tangential velocity
Um	Local mean bulk velocity
Umax	Local maximum velocity at the 90 degree location
Ur	Local mean radial velocity
U_τ	Shear stress velocity, $\sqrt{\tau_w/\rho}$
$\overline{uv}$	Reynolds turbulent stress
v′	Root-mean-square of the radial turbulent velocity
w′	Root-mean-square of the lateral turbulent velocity
x	Tangential distance along the duct
y	Radial distance from the inner wall of the duct
y′	Radial distance from the outer wall of the duct
α	Angle between the mean flow and the tangential direction
δ	Laminar boundary layer thickness, taken as point of Umax
ρ	Water density
τ_w	Surface shear stress

TABLE I. STATIC PRESSURE DISTRIBUTION

Location inner wall	Re	Cp
-5.33cm	738,000	-.0708
	826,000	-.0689
	950,000	-.0652
10.55deg	531,000	-1.371
	664,000	-1.509
	761,000	-1.529
	864,500	-1.496
	898,000	-1.513
28.3 deg	721,000	-2.006
	817,000	-2.006
	907,000	-1.941
50.5 deg	745,000	-2.435
	827,000	-2.406
	919,000	-2.382
70.9 deg	740,000	-2.446
	850,000	-2.320
	906,000	-2.387
110.5deg	672,000	-2.129
	794,000	-2.216
	859,000	-2.189
	919,000	-2.221
130.4deg	726,000	-1.748
	823,000	-1.746
	920,000	-1.804
150.5deg	728,000	-1.365
	825,000	-1.413
	924,000	-1.446
170.8deg	703,500	-0.783
	828,000	-0.756
	927,000	-0.748
+6.86cm	714,000	-0.538
	734,000	-0.543
	832,000	-0.541
	834,000	-0.521
	942,000	-0.522
	946,000	-0.523

Location outer wall	Re	Cp
-84.8cm	666,000	-.00019
	796,000	+.00006
	896,000	+.00023
-60.7cm	719,000	+.00080
	808,000	+.00002
	911,000	+.00052
-36.8cm	711,000	-.00164
	796,000	-.00127
	894,000	-.00068
-17.5cm	721,000	-.0119
	804,000	-.00887
	907,000	-.00583
9.9 deg	666,000	+0.243
	796,000	0.243
	896,500	0.267
30.1deg	719,000	0.319
	808,000	0.336
	911,000	0.344
50.2deg	711,000	0.356
	796,000	0.364
	895,000	0.369
70.3deg	721,000	0.361
	804,000	0.369
	907,000	0.378
110.4deg	732,000	0.363
	819,000	0.383
	920,000	0.374
130.5deg	733,000	0.352
	822,000	0.360
	916,000	0.369
150.6deg	733,000	0.256
	824,000	0.268
	919,000	0.376
170.8deg	728,000	0.156
	827,000	0.172
	908,000	0.173
7.94cm	712,000	-0.415
	819,000	-0.411
	939,000	-0.406
17.3cm	723,000	-0.287
	817,000	-0.289
	941,000	-0.282

b) Extrapolated values of Cp

Location	Reynolds Number			
inner wall	700,000 Cp	800,000 Cp	900,000 Cp	1,000,000 Cp
-5.33cm	-.0718	-.0694	-.0669	-.0643
10.55deg	-1.510	-1.511	-1.513	-1.517
28.3 deg	-2.012	-1.997	-1.977	-1.960
50.5 deg	-2.448	-2.420	-2.388	-2.358
70.9 deg	-2.457	-2.424	-2.392	-2.358
110.5deg	-2.149	-2.173	-2.208	-2.273
130.4deg	-1.707	-1.741	-1.790	-1.851
150.5deg	-1.353	-1.398	-1.437	-1.480
170.8deg	-0.781	-0.760	-0.748	-0.745
+6.86cm	-0.540	-0.533	-0.525	-0.513
outer wall				
-84.8cm	0	+.00006	+.00023	
-60.7cm	+.0008	+.00010	+.00052	
-36.8cm	-.0020	-.0010	-.0003	
-17.5cm	-.0127	-.0090	-.0062	-.0043
9.9 deg	+0.246	+0.256	+0.268	+0.278
30.1 deg	+0.314	+0.334	+0.344	+0.350
50.2 deg	+0.355	+0.364	+0.369	+0.372
70.3 deg	+0.358	+0.368	+0.376	+0.382
110.4deg	+0.364	+0.375	+0.383	+0.389
130.5deg	+0.348	+0.358	+0.368	+0.371
150.6deg	+0.251	+0.265	+0.277	+0.283
170.8deg	+0.156	+0.166	+0.174	+0.179
+6.86cm	-0.416	-0.412	-0.410	-0.403
+17.3cm	-0.287	-0.287	-0.287	-0.287

TABLE II. VELOCITY FIELD MEASUREMENTS

a) Upstream inlet (-101.6cm)

$T = 10.2^{\circ}$ C

$\rho = .9997 gm/cm^3$

$\nu = 1.305 \times 10^{-6}$ m^2/sec

y cm	Re	Ut m/sec	u' m/sec	Ur m/sec	α deg	v' m/sec	$\overline{uv}$ (m/sec)
.102	532,000	5.712	.3892				
	664,000	7.577	.4490				
	762,000	9.016	.3776				
	854,000	10.30	.5980				
	899,000	10.81	.5700				
.305	721,000	9.065	.5066				
	818,000	10.47	.5371				
	908,000	11.70	.5099				
.762	745,000	9.903	.3203				
	827,000	10.97	.3240				
	921,000	12.21	.3044				
1.52	740,000	9.891	.2161	-.249	-1.442	.3533	-.04607
	838,000	11.17	.2646	-.112	-0.572		-.00826
	907,000	12.08	.2382				
6.35	672,000	8.995	.1844	+.019	+0.121	.1877	+.00567
	794,000	10.58	.1827	+.005	+0.026	.2299	+.00233
	861,000	11.43	.1936	+.092	+0.464	.2284	+.00319
	921,000	12.18	.2014				
9.53	728,000	9.165	.5060				
	826,000	10.64					
9.78	741,000	8.644	.6419				
	799,000	9.357	.6593				
	910,000	10.59	.6151				
9.91	718,000	7.940	.6623				
	811,000	9.107	.6937				
	919,000	10.72	.8522				

c) Start of the turn

$T = 8.8^{\circ}C$

$\rho = .9998$ gm/cm^3

$\nu = 1.356 \times 10^{-6} m^2/sec$

y cm	Re	Ut m/sec	u' m/sec	Ur m/sec	α deg	v' m/sec	$\overline{uv}$ (m/sec)
.140	398,000	6.584	.229				
	587,000	10.94	.448				
	725,000	13.18	.680				
	809,000	14.32	.789				
.508	624,000	11.20	.262				
	740,000	13.09	.503				
	835,000	15.55	.314				
1.27	605,000	10.57	.235	-2.298	-12.27	.0924	-.0111
	725,000	12.43	.308	-2.691	-12.22		-.0136
	813,000	13.89	.363	-2.990	-12.15	.256	-.0169
2.54	621,000	9.885	.186				
	711,000	11.23	.196				
	820,000	12.93	.348				
4.99	590,000	8.321	.216	-2.118	-14.28		+.00431
	708,000	9.793	.211	-2.481	-14.22	.243	+.00733
	829,000	11.34	.29	-2.822	-13.98		+.00539
7.62	625,000	7.300	.145	-1.484	-11.49	.118	-.00106
	749,000	8.705		-1.969	-12.75	.154	-.00431
	831,000	9.687		-1.841	-10.76	.129	+.00200
9.14	622,000	5.532					
	748,000	6.593					
	835,000	7.559					
9.40	637,000	5.233					
	750,000	6.035					
	834,000	6.885					
9.65	635,000	4.478					
	749,000	5.191					
	836,000	6.011					

Repeat run ($T = 6.3^{\circ}C$)

7.62	612,000	8.099	.3088
	716,000	9.415	.3426
	793,000	10.39	.3048
9.14	625,000	6.367	.5127
	699,000	7.145	.7245

b) -17cm upstream of the turn

$T = 9.5^{\circ}C$

$\rho = .9998 gm/cm^3$

$\nu = 1.334 \times 10^{-6} m^2/sec$

y cm	Re	Ut m/sec	u' m/sec
.203	505,000	5.944	.4002
	608,000	7.276	.4107
	701,000	8.202	.5931
	772,000	9.193	.6175
	840,000	10.19	.6072
.305	442,000	5.483	.3472
	567,000	6.754	.3862
	660,000	8.352	.3979
	772,000	9.461	.5873
	847,000	10.47	.5928
.508	487,000	6.154	.3523
	615,000	7.843	.5371
	767,000	9.659	.5944
	835,000	10.76	.5422
1.07	464,000	6.398	.1791
	619,000	8.547	.2060
	735,000	9.815	.3249
	792,000	10.69	.3225
	844,000	11.52	.3051
2.34	473,000	6.553	.1177
	587,000	7.980	.1062
	665,000	9.528	.1855
	772,000	10.73	.1988
	851,000	11.73	.2352
4.97	451,000	6.425	.1254
	596,000	8.025	.1149
	651,000	9.431	.1242
	774,000	10.80	.1390
	836,000	11.77	.1843
7.42	510,000	7.117	.2432
	619,000	8.583	.2882
	731,000	9.842	.2927
	792,000	10.77	.2890
	840,000	11.51	.2844
8.94	460,000	5.581	.3822
	574,000	6.971	.4279
	655,000	8.160	.5784
	767,000	9.351	.5944
	842,000	10.39	.6203
9.76	423,000	4.054	.4898
	564,000	5.483	.4846
	649,000	6.468	.5404
	776,000	7.477	.5712
	845,000	8.208	.6014
9.81	423,000	3.905	.4886
	567,000	5.325	.5163
	658,000	6.373	.7489
	778,000	7.285	.8028
	844,000	8.190	.7498
9.86	401,000	3.143	.3304
	576,000	5.026	.5240
	660,000	5.742	.6035
	781,000	6.294	.6053
	835,000	7.090	.5538
9.91	437,000	3.210	.3423
	549,000	4.197	.3807
	626,000	4.953	.4474
	733,000	5.590	.8665
	792,000	5.947	.9214
	831,000	5.806	.9587

TABLE II. (CONCLUDED) VELOCITY FIELD MEASUREMENTS

d) 90 degrees around the turn
T = 9.0°C
ρ = .9999gm/cm^3
ν = 1.355x10^{-6}m^2/sec

y cm	Re	Ut m/sec	u' m/sec	Ur m/sec	α deg	v' m/sec	$\overline{uv}$ (m/sec)
.051	573,000	13.54					
	662,000	15.92	.6410				
	736,000	17.71	.5919				
	803,000	18.33	.8095				
.102	596,000	14.49	.2880?				
	713,000	16.98	.6895				
	824,000	18.09	.9467				
.203	596,000	14.50	.3920				
	724,000	17.54	.4295				
	825,000	19.47	.5230				
.381	602,000	14.50	.4103				
	722,000	17.27	.4346				
	827,000	19.48	.4889				
.965	627,000	14.17	.4054	0.381	+1.541		-.00900
	724,000	16.23	.4901	0.268	+0.947		+.00971
	819,000	18.06	.3917	0.608	+1.991	.4910	+.02191
2.34	607,000	9.571	.1838	0.327	-1.789	.2423	+.01103
	737,000	8.449	.2966	0.581	+2.472	.3649	+.02652
	833,000	14.94	.3630	0.744	+2.852	.3630	+.03406
4.98	635,000	7.797	.6456	0.258	+1.898		+.1427
	736,000	9.144	.6370	0.491	+3.072	.7931	+.2627
	845,000	10.58	.5584	0.515	+2.783	.9275	+.3011
7.62	627,000	5.471		-.012	-.124	.8300	+.1683
	724,000	6.343		+.012	+.107	1.427	+.8318
	820,000	7.151		0.265	+2.127	1.448	+.5385
8.64	628,000	4.551					
	737,000	5.755					
	839,000	6.431					
9.14	618,000	4.837					
	736,000	5.715					
	835,000	6.206					

Repeat run (T = 6.1°C)

7.62	595,000	5.788	.9211
	687,000	6.843	1.348
	760,000	7.321	1.177
8.89	593,000	5.124	.8425
	680,000	5.846	.8358
	763,000	6.514	.9613
9.27	599,000	5.148	.8693
	687,000	5.435	.8665
	701,000	5.916	.830

e) Exit of the turn (above the separation bubble)
T = 10.6°C
ρ = .9997gm/cm^3
ν = 1.294x10^{-6}m^2/sec

y cm	Re	Ut m/sec	u' m/sec	Ur m/sec	α deg	v' m/sec	$\overline{uv}$ (m/sec)
1.02	714,000	0.286					
	834,000	0.356					
	942,000	0.436					
1.52	738,000	10.34	1.024	6.184	30.88	.4075	+.4814
	826,000	11.54	1.210	6.236	28.38	.3009	+.4360
	949,000	12.51	.6477	6.474	27.35	.9873	+.2637
2.03	723,000	11.72	.5934	6.111	27.55	.8169	+.2269
	817,500	13.47	.5179	7.242	28.26	.5685	+.00756
	941,000	14.97	1.018	8.394	29.28	.4110	+.2893
3.03	712,000	11.37	.3853	5.611	26.27	.5212	+.03243
	819,000	12.84	.7087	6.102	25.43	.7998	+.1499
	939,000	14.55	.7312	7.141	26.14		-.06552
4.99	710,000	10.88	.4426	4.161	20.96	.8922	-.02282
	828,000	12.42	.7007	4.819	21.22	1.102	+.1638
	927,000	13.77	.7300	5.340	21.19	1.074	+.2067
7.67	725,000	9.851	.5834	2.527	14.39	1.527	-.1133
	819,000	11.13	.5538	3.191	15.99	1.465	-.09541
	930,000	12.64	.5630	3.389	15.01	1.655	-.2226
8.99	723,000	9.501	.5642	1.502	8.982	1.355	-.1109
	819,000	10.79	.5822	4.935	24.58	1.371	-.1123
	928,000	12.17	.6114	5.621	24.79	1.287	-.1014
9.37	725,000	9.385	.5599				
	828,000	10.67	.5721				
	915,000	11.96	.6910				
9.62	725,000	9.315	.5767				
	821,000	10.63	.5709				
	941,000	12.06	.5956				
9.80	710,000	9.616	.5566				
	815,000	11.06	.5773				
	925,000	12.49	.6306				

f) +3.06H downstream of the turn
T = 10.4°C
ρ = .9997gm/cm^3
ν = 1.303x10^{-6}m^2/sec

y cm	Re	Ut m/sec	u' m/sec	Ur m/sec	α deg	v' m/sec	$\overline{uv}$ (m/sec)
.102	665,000	4.770	1.355				
	795,000	5.172	1.347				
.254	717,000	5.520	1.573				
	809,000	5.803	1.618				
	912,000	7.215	1.364				
1.02	711,000	5.928					
	799,000	6.922	1.602	+.588	+4.857		-.9950
	897,000	8.086	2.149	-.833	-5.883		-1.228
2.03	721,000	7.495	2.059	-.292	-2.228		-1.005
	804,000	7.864	2.274	-.524	-3.812		-.6130
	908,000	8.632	2.486	+.088	+0.582		-1.147
2.54	733,000	8.693	1.918	-.287	-1.890		-1.577
	826,000	8.681	2.220	-.450	-2.971	.6891	-.6885
	924,000	10.18	2.108	+.007	+0.040	1.610	-.9035
3.81	731,000	9.022	1.938	-.228	-1.445		
	821,000	9.979	2.092	-.758	-3.820	1.918	-1.666
	921,000	10.99	2.123				
4.99	732,000	10.10	1.700	-.261	-1.479	4.362	-2.405
	824,000	11.24	1.761	-.752	-3.825		
	917,000	12.31	1.920	-.368	-1.710	1.736	-.3142
7.37	732,000	11.34	1.152	-.123	-0.623	1.723	+.1311
	826,000	12.66	1.189	-.123	-0.558	1.738	+.0190
	920,000	13.80	1.972	-.178	-0.738	1.151	+1.031
9.58	727,000	11.44	1.099				
	828,000	12.63	1.873				
	904,000	13.84	1.854				
9.84	730,000	11.28	1.167				
	821,000	12.67	1.162				
	917,000	14.13	1.194				

TABLE III. EXTRAPOLATED MEAN AND TURBULENT VELOCITY PROFILES

a) Upstream inlet (-101.6cm)

	Re = 700,000		800,000		900,000		980,000
	Um = 9.138m/s		10.44m/s		11.75m/s		12.79m/s
y/H	U/Um	u'/Um	U/Um	u'/Um	U/Um	u'/Um	U/Um
.0102	.886	.05220	.9113	.05263	.9284	.04829	.9376
.0305	.9566	.05330	.9752	.05333	.9865	.04442	.9905
.0762	1.016	.03412	1.017	.03103	1.016	.02621	1.015
0.152	1.025	.01955	1.022	.02428	1.022	.02068	1.020
0.610	1.025	.0199	1.018	.0176	1.015	.0169	1.011
0.838	1.072		1.047		1.028		1.014
0.953	.9566		.9813		.9935		.9974
0.979	.8799	.06731	.8984	.06311	.9165	.05301	
0.991	.8409	.07128	.8669	.06623	.8874	.05646	.8997

b) -17cm upstream of the turn

	Re = 600,000		700,000		800,000		850,000	
	Um = 8.035m/s		9.374m/s		10.71m/s		11.38m/s	
y/H	U/Um	u'/Um	U/Um	u'/Um	U/Um	u'/Um	U/Um	u'/Um
.0204	.8896	.0508	.8771	.0630	.8947	.0579	.9545	.0531
.0306	.9416	.0478	.9168	.0539	.9183	.0552	.9687	.0521
.0510	.9522	.0580	.9379	.0632	.9482	.0539	1.009	.0466
0.112	1.026	.0240	.9993	.0251	1.006	.0300	1.069	.0266
0.240	1.043	.0141	1.038	.0196	1.034	.0194	1.077	.0249
0.501	1.076	.0147	1.057	.0131	1.049	.0147	1.092	.0170
0.750	1.041	.0346	1.020	.0311	1.020	.0270	1.068	.0250
0.903	.9112	.0579	.9021	.0635	.9127	.0561	.9617	.0542
0.984	.7367	.0620	.7373	.0590	.7260	.0542	.7451	.0530
0.989	.7102	.0717	.7139	.0845	.6962	.0735	.7127	.0655
0.994	.6495	.0683	.6460	.0662	.6356	.0551	.6525	.0475
0.999	.5827	.0519	.5774	.0662	.5593	.0867	.5663	.0855

c) Start of the turn

	Re = 600,000		700,000		800,000		850,000	
	Um = 8.138m/s		9.495m/s		10.85m/s		11.53m/s	
y/H	U/Um	u'/Um	U/Um	u'/Um	U/Um	u'/Um	U/Um	u'/Um
.014	1.370	.0576	1.352	.0692	1.312	.0711	1.285	.0709
.0510	1.328	.0281	1.308	.0432	1.343		1.392	
0.128	1.286	.0284	1.272	.0308	1.262	.0297	1.260	.0333
0.255	1.175	.0235	1.170	.0203	1.166	.0288	1.165	.0351
0.501	1.013	.0257	1.026	.0221	1.014	.0246	1.005	.0271
0.765	0.810		0.848		0.864		0.857	
0.918	0.655		0.651		0.661		0.672	
0.943	0.612		0.598		0.603		0.613	
0.969	0.525		0.513		0.522		0.535	

d) 90 degrees around the turn

	Re = 600,000		700,000		800,000		850,000	
	Um = 8.126m/s		9.482m/s		10.84m/s		11.51m/s	
y/H	U/Um	u'/Um	U/Um	u'/Um	U/Um	u'/Um	U/Um	u'/Um
.0052	1.77		1.79	.0485	1.70	.0731	1.61	.0802
.010	1.81	.0381	1.82	.0659		.0816		.0865
.021	1.81	.0484	1.81	.0443	1.78	.0451	1.72	.0492
.0388	1.79	.0501	1.78	.0452	1.78	.0435	1.74	.0440
.0983	1.68	.0444	1.67	.0487	1.66	.0449	1.62	.0272
0.238	1.33	.0217	1.36	.0283	1.36	.0314	1.33	.0323
0.509	0.908	.0799	0.921	.0675	0.932	.0554	0.935	.0480
0.776	0.645	.0748	0.654	.0769	0.651	.0694	0.643	.0652
0.880		.0762	0.585	.0668	0.578	.0615	0.567	.0609
0.931	0.581	.0767	0.580	.0668	0.564	.0619	0.546	.0619

e) Exit of the turn

	Re = 700,000		800,000		900,000		1,000,000
	Um = 9.094m/s		10.39m/s		11.69m/s		12.99m/s
y/H	U/Um	u'/Um	U/Um	u'/Um	U/Um	u'/Um	U/Um
0.153	1.06	.0958	1.08	.117	1.04	.0778	0.995
0.204	1.24	.0700	1.27	.0490	1.24	.0696	1.21
0.332	1.24	.0382	1.21	.0646	1.20	.0633	1.19
0.749	1.05	.0636	1.05	.0577	1.05	.0524	1.04
0.902	1.01	.0616	1.01	.0558	1.01	.0515	1.00
0.940	1.01	.0612	0.995	.0548	1.00	.0508	1.02
0.966	0.992	.0636	0.997	.0551	0.988	.0499	0.978

f) +3.06H downstream of the turn

	Re = 700,000		800,000		900,000		950,000
	Um = 9.092m/s		10.39m/s		11.69m/s		12.34m/s
y/H	U/Um	u'/Um	U/Um	u'/Um	U/Um	u'/Um	U/Um
.010	0.530	0.149	0.506	0.130		0.114	
.0255	0.600	0.171	0.560	0.155	0.623	0.126	0.662
0.102	0.682	0.167	0.648	0.155	0.658	0.174	0.744
0.204	0.810	0.220	0.760	0.217	0.772	0.211	0.788
0.255	0.852	0.200	0.818	0.205	0.850	0.186	0.872
0.383	0.955	0.205	0.946	0.198	0.941	0.181	0.939
0.501	1.07	0.184	1.06	0.168	1.06	0.161	1.05
0.739	1.20	0.128	1.19	0.133	1.18	0.133	1.17
0.961	1.22		1.19		1.19		1.20
0.987	1.20	0.128	1.19	0.113	1.20	0.102	1.20

TABLE IV. VELOCITY MEASUREMENTS IN THE SEPARATION BUBBLE

a) 170 degrees around the turn

$T = 8.4^{\circ}$ C

$\rho = .9999 gm/cm^3$

$\nu = 1.365 \times 10^{-6}$ m^2/sec

y cm	Re	Ut m/sec	u' m/sec
.102	413,000	-0.150	0.969
	677,000	-0.527	1.03
	801,000	-0.248	0.951
.254	724,000	-0.463	1.40
	837,000	-.0780	0.735
.381	713,000	+0.570	1.09
	835,000	0.408	1.20
.635	716,000	2.40	3.35
	816,000	1.89	3.29
	890,000	1.27	2.74

b) 180 degrees aroun the turn

$T = 8.8^{\circ}$ C

$\rho = .9999 gm/cm^3$

$\nu = 1.352 \times 10^{-6}$ m^2/sec

y cm	Re	Ut m/sec	u' m/sec
.102	436,000	-0.732	0.914
	436,000	-0.704	0.887
	544,000	-0.750	1.11
	776,000	-0.689	1.11
	837,000	-0.518	1.41
	836,000	-0.832	1.27
.318	596,000	-0.597	1.32
	723,000	-0.634	1.56
	748,000	-0.671	1.56
	771,000	-0.491	1.55
.445	623,000	-.0332	1.15
	696,000	+.0564	1.19
	781,000	+0.254	1.39
.762	601,000	1.63	2.51
	696,000	1.41	2.56
	755,000	1.11	2.55
1.02	605,000	3.35	3.20
	672,000	3.80	3.69
	788,000	4.10	4.05
4.99	620,000	8.81	
	710,000	10.1	1.0
	777,000	10.9	1.2

c) 5.08cm downstream of the turn

$T = 8.7^{\circ}$ C

$\rho = .9999 gm/cm^3$

$\nu = 1.352 \times 10^{-6}$ m /sec

y cm	Re	Ut m/sec	u' m/sec
.152	429,000	-0.689	1.07
	606,000	-0.658	1.16
	696,000	-0.518	1.36
	814,000	-1.43	0.546
.254	634,000	-1.59	1.23
	723,000	-1.12	1.17
	798,000	-0.436	1.45
	832,000	-1.03	0.725
.508	594,000	-1.28	1.45
	686,000	-1.23	1.52
	798,000	-0.858	1.54
.762	576,000	-0.913	1.71
	705,000	-0.701	1.88
	802,000	-1.03	1.89
	840,000	-0.320	1.58
1.27	607,000	-0.155	1.79
	708,000	+0.335	2.09
	822,000	0.666	2.27
	864,000	0.936	2.04
1.78	619,000	2.05	3.04
	703,000	2.26	3.35
	799,000	2.97	3.32
	837,000	3.41	3.69
2.54	614,000	6.16	3.08
	697,000	7.01	3.60
	809,000	7.80	3.90
	873,000	7.86	4.16
Repeat	Run (T = 8.6 C)		
.381	679,000	-1.17	1.56
	823,000	-0.692	1.77
	823,000	-0.844	1.64
	870,000	-0.599	1.89
1.02	677,000	+.0564	2.25
	823,000	0.622	2.54
	897,000	1.28	2.55
4.98	694,000	12.4	0.860
	801,000	14.2	0.79
	874,000	15.5	0.95

d) 7cm downstream of the turn

$T = 8.4^{\circ}$ C

$\rho = .9999 gm/cm^3$

$\nu = 1.365 \times 10^{-6}$ m^2/sec

y cm	Re	Ut m/sec	u' m/sec
.076	505,000	-1.26	1.31
	745,000	-1.11	1.65
	805,000	-0.890	1.65
	890,000	-0.150	1.45
.152	449,000	-1.07	1.13
	699,000	-1.13	1.77
	808,000	-0.832	1.69
	897,000	-0.281	0.937
.254	703,000	-0.820	1.84
	808,000	-0.820	1.87
	881,000	-0.482	1.95
.508	694,000	-0.338	2.22
	819,000	-.0332	2.18
	881,000	+0.378	2.43
.762	687,000	0.604	2.55
	792,000	0.917	2.69
	868,000	1.20	2.73
1.27	721,000	2.50	2.92
	830,000	2.52	3.05
	890,000	3.20	3.41

TABLE V. EXTRAPOLATED MEAN AND TURBULENT VELOCITY PROFILES IN THE SEPARATION BUBBLE

a) 170 degrees around the turn

	Re = 600,000		700,000		800,000		850,000	
	Um = 8.22m/s		9.59m/s		11.0m/s		11.6m/s	
$\frac{y}{H}$	$\frac{U}{Um}$	$\frac{u'}{Um}$	$\frac{U}{Um}$	$\frac{u'}{Um}$	$\frac{U}{Um}$	$\frac{u'}{Um}$	$\frac{U}{Um}$	$\frac{u'}{Um}$
.010	-0.0741	0.126	-0.0524	0.106	-0.0239	0.0867	+0.002	0.0780
.025	-0.0741		-0.0524	0.113	-0.0239	0.892	+0.002	0.0604
.038	-0.0826	0.132	-0.0619	0.156	-0.0375	0.103	-0.0281	0.106
.064	+0.333	0.411	+0.255	0.350	+0.182	0.301	+0.140	0.269

b) 180 degrees around the turn

	Re = 600,000		700,000		800,000	
	Um = 8.14m/s		9.50m/s		10.9m/s	
$\frac{y}{H}$	$\frac{U}{Um}$	$\frac{u'}{Um}$	$\frac{U}{Um}$	$\frac{u'}{Um}$	$\frac{U}{Um}$	$\frac{u'}{Um}$
.010	-0.0925	0.138	-0.0760	0.118	-0.0562	0.107
.0319	-0.0734	0.162	-0.0660	0.149	-0.0435	0.158
.0446	-0.0067	0.139	+0.0064	0.127	+0.0298	0.134
.0765	+0.200	0.308	0.139	0.269	0.0969	0.230
.102	0.408	0.371	0.409	0.395	0.387	0.413
.501	1.04	0.0831	1.01	0.104	1.06	0.112

c) 5.08cm downstream of the turn

	Re = 600,000		700,000		800,000		850,000	
	Um = 8.14m/s		9.50m/s		10.9m/s		11.5m/s	
$\frac{y}{H}$	$\frac{U}{Um}$	$\frac{u'}{Um}$	$\frac{U}{Um}$	$\frac{u'}{Um}$	$\frac{U}{Um}$	$\frac{u'}{Um}$	$\frac{U}{Um}$	$\frac{u'}{Um}$
.015	-0.0820	0.142	-0.0548	0.143	-0.02	0.142		
.026		0.145		0.140		0.134		0.129
.038	-0.155	0.185	-0.122	0.169	-0.0815	0.160	-0.0587	0.159
.051	-0.158	0.179	-0.127	0.160	-0.0809	0.143	-0.0563	0.135
.077	-0.107	0.214	-0.0747	0.241	+0.0449	0.230	-0.0087	0.162
.102	-0.0105	0.252	+0.0119	0.241	0.0449	0.230	+0.0773	0.222
.128	+0.018	0.217	0.0337	0.217	0.0542	0.208	0.0746	0.198
.179	0.246	0.363	0.238	0.350	0.274	0.334	0.309	0.322
.255	0.775	0.366	0.739	0.374	0.713	0.360	0.697	0.354
.500	1.28	0.0712	1.43	0.0676	1.31	0.0725	1.31	0.0765

d) 7cm downstream of the turn

	Re = 600,000		700,000		800,000		900,000	
	Um = 8.22m/s		9.59m/s		11.0m/s		12.3m/s	
$\frac{y}{H}$	$\frac{U}{Um}$	$\frac{u'}{Um}$	$\frac{U}{Um}$	$\frac{u'}{Um}$	$\frac{U}{Um}$	$\frac{u'}{Um}$	$\frac{U}{Um}$	$\frac{u'}{Um}$
.0076	-0.173	0.202	-0.128	0.172	-0.0828	0.150	-0.0330	0.115
.015	-0.159	0.223	-0.117	0.184	-0.0778	0.154	-0.0213	0.0748
.026	-0.103	0.228	-0.0873	0.192	-0.0758	0.170	-0.0282	0.161
.051	-0.0574	0.272	-0.0340	0.230	-0.0089	0.199	+0.0449	0.207
.077	+0.0444	0.284	+0.0657	0.261	+0.0861	0.245	0.108	0.224
.128	0.301	0.336	0.260	0.301	0.232	0.274	0.276	0.285

TABLE VI. SURFACE SHEAR STRESS MEASUREMENTS

a) -17cm upstream of the turn
T = 9.5°C
ρ = .9998gm/cm^3
ν = 1.334x10^{-6} m^2/sec

Re	Um m/sec	U_τ/Um
437,000	5.85	.0350
549,000	7.35	.0355
626,000	8.38	.0357
733,000	9.81	.0341
792,000	10.6	.0333
831,000	11.1	.0328
401,000	5.36	.0341
576,000	7.71	.0357
660,000	8.84	.0355
781,000	10.5	.0334
835,000	11.2	.0329
423,000	5.67	.0350
567,000	7.59	.0356
658,000	8.81	.0356
778,000	10.4	.0335
844,000	11.3	.0327
423,000	5.67	.0350
564,000	7.56	.0355
649,000	8.69	.0356
776,000	10.4	.0335
845,000	11.3	.0327

b) 10 degrees around the turn
T = 9.5°C
ρ = .9998gm/cm^3
ν = 1.334x10^{-6} m^2/sec

Re	Um m/sec	U_τ/Um
457,000	6.10	.0203
576,000	7.69	.0190
657,000	8.77	.0185
755,000	10.1	.0176
840,000	11.2	.0164
509,000	6.79	.0188
620,000	8.27	.0181
718,000	9.58	.0178

c) 90 degrees around the turn
(same properties as above)

Re	Um m/sec	U_τ/Um
450,000	6.01	.0264
471,000	6.28	.0268
590,000	7.87	.0255
664,000	8.86	.0270
761,000	10.2	.0267
847,000	11.3	.0267
461,000	6.15	.0278
622,000	8.30	.0268
723,000	9.64	.0271
782,000	10.4	.0274
841,000	11.2	.0273

d) 130 degrees around the turn
(same properties as above)

Re	Um m/sec	U_τ/Um
443,000	5.91	.0336
568,000	7.58	.0318
662,000	8.23	.0336
760,000	10.1	.0334
843,000	11.3	.0326

TABLE VII. EVALUATION OF THE LATERAL TURBULENT VELOCITY

a) 50 degrees around the turn
T = 9.4° C
$\nu = 1.336 \times 10^{-6}$ m^2/sec

y/H	Re	U	u'	w'	v'	$\overline{uv}$	Ur	α
		m/s	m/s	m/s	m/s	(m/s)	m/s	deg
.021	506,000	4.069	1.05	1.02				
	665,000	5.355	1.12	1.08				
	782,000	6.279	1.37	1.52				
.052	421,000	3.28	.817	.747				
	533,000	3.82	1.19	.878				
.103	419,000	3.54	.829	.789				
	531,000	5.03	1.15	1.20				
	618,000	6.07	1.28	1.10		.827	.223	2.10
.155	464,000	3.72	.817	.750	.669	.393	.023	0.25
	564,000	5.49	1.25	1.23	1.41	1.33	.710	6.05
	649,000	6.67	1.32	1.22	1.03	.849	.284	4.37
.207	450,000	3.84	.805	.640		.188	.558	8.25
	567,000	6.07	1.20	1.18	.908	.753	.485	4.58
	645,000	7.19	1.36	1.16	.802	.718	.972	7.70
.310	405,000	3.90	.466	.555		.0458	.314	4.62
	470,000	5.61	.719	.622	.860	.161	.402	4.11
	558,000	7.22	.975	1.34	1.47	.411	.357	2.82
	661,000	9.21	1.04	1.14	.988	.255	.521	3.24
.414	432,000	5.27	.442	.424		.192	.095	1.03
	543,000	7.43	.927	.43				
	611,000	9.45	.634	1.02	.997	.597	1.90	11.4

b) 90 degrees around the turn
T = 9.4° C
$\nu = 1.366 \times 10^{-6}$ m^2/sec

y/H	Re	U	u'	w'
		m/s	m/s	m/s
.032	421,000	3.08	.533	.863
	542,000	3.95	.649	.942
	707,000	5.14	.85	1.9
.103	497,000	3.78	.616	.677
	567,000	4.33	.707	.485
	647,000	4.94	.81	1.3
.207	405,000	3.32	.546	1.27
	520,000	4.40	.725	.792
	654,000	5.76	.777	2.28

c) 130 degrees around the turn
T = 9.4° C
$\nu = 1.336 \times 10^{-6}$ m^2/sec

y/H	Re	U	u'	w'	v'	$\overline{uv}$	Ur	α
		m/s	m/s	m/s	m/s	(m/s)	m/s	deg
.026	413,000	2.41	.344	.61				
	459,000	3.32	.439	.49				
	571,000	4.60	.582	.79				
	625,000	5.24	.555					
.103	459,000	3.29	.439	.82				
	517,000	4.08	.564	.67	.668	.132	.190	2.66
	614,000	5.36	.582		.890	.190	.024	0.25
.207	428,000	3.14	.421	1.1	.536	.076	.137	2.51
	546,000	4.97	.555		1.07	.231	.308	3.55
	609,000	5.67	.664					
.310	470,000	4.42	.546	.73	.884	.261	.237	3.07
	587,000	5.97	.664	.58	.683	.146	.521	4.99
.414	477,000	4.08	.527	1.7	.887	.269	.261	3.65
	611,000	6.98	.744	1.5	1.02	.423	.451	2.17
.492	408,000	3.75	.384					
	520,000	5.97	.527	.73	.695	.177	.378	3.61
	596,000	7.29	.582		.905	.349	.497	3.91

130 degrees with film probe

.026	396,000	.866
	403,000	.924
	493,000	.860
	562,000	.860
	580,000	.924
	589,000	1.08
.103	479,000	.671
	564,000	.707
	609,000	.936
.207	387,000	.725
	526,000	.521
	609,000	1.06

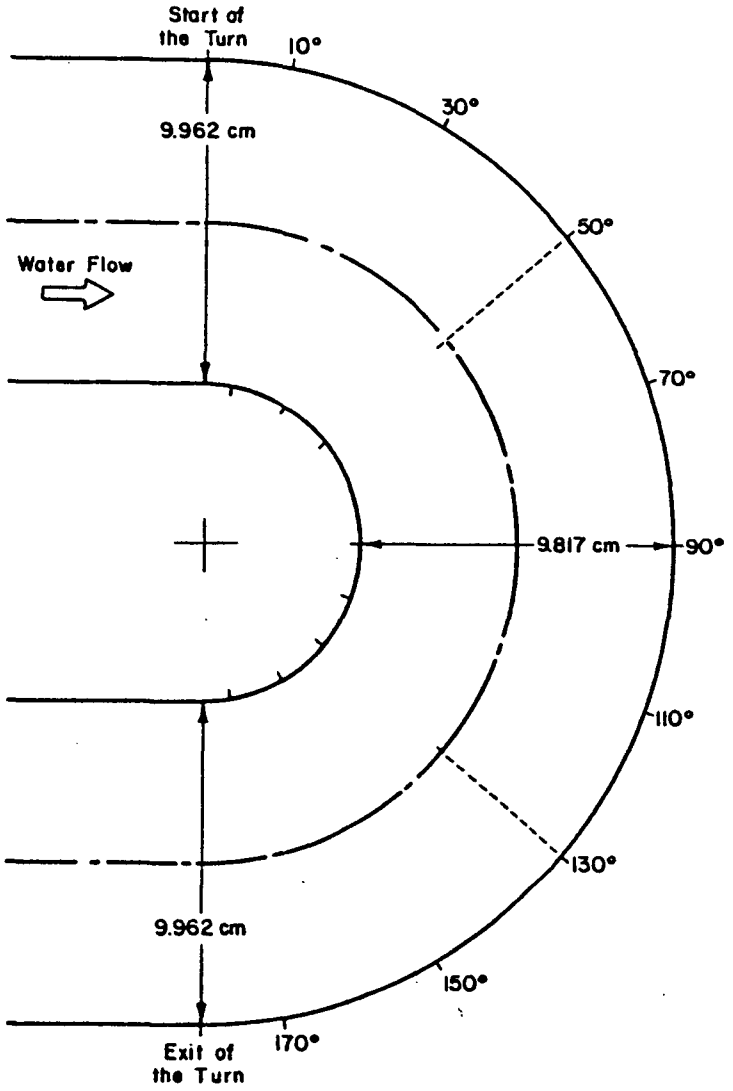

Dimensions for present tests.

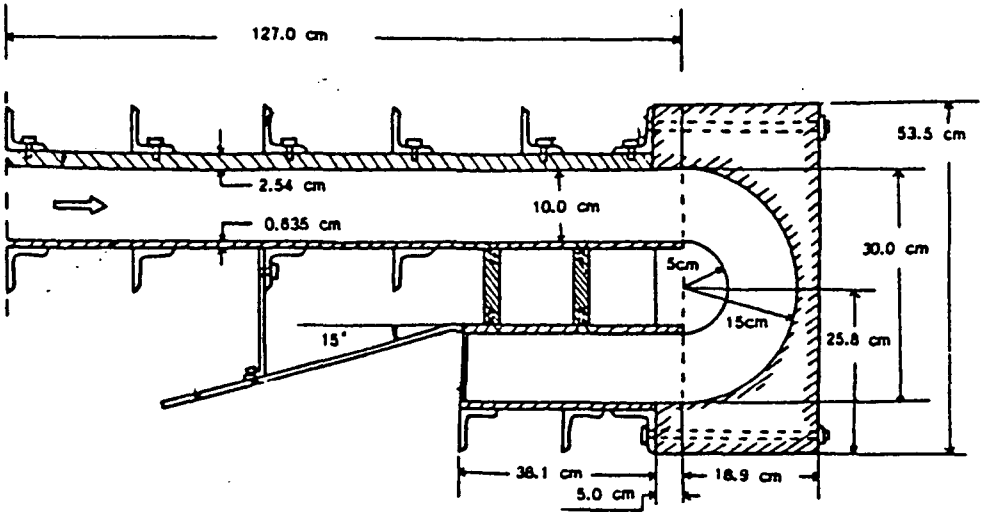

Construction dimensions

Figure 1. Turn-around-duct.

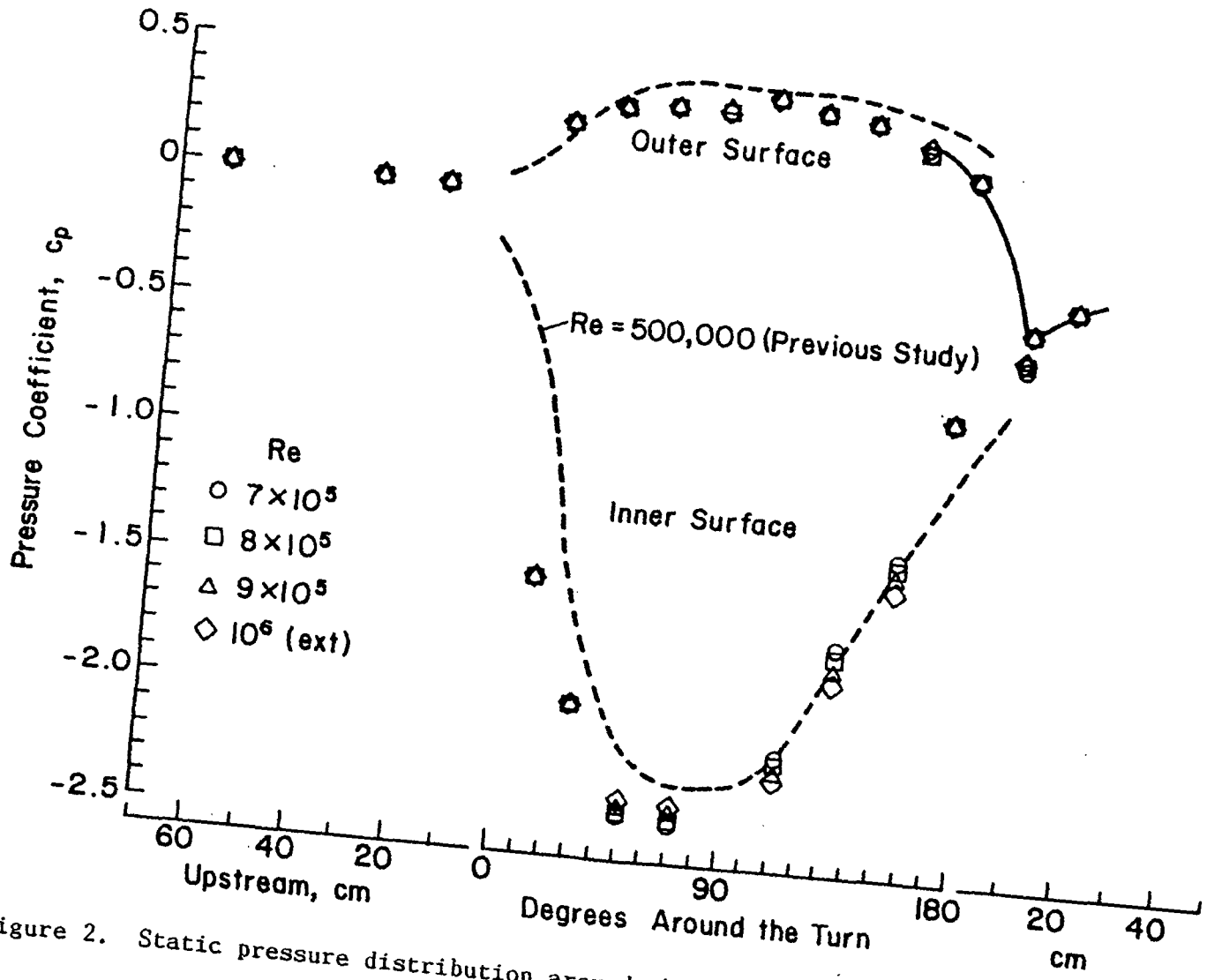

Figure 2. Static pressure distribution around the turn.

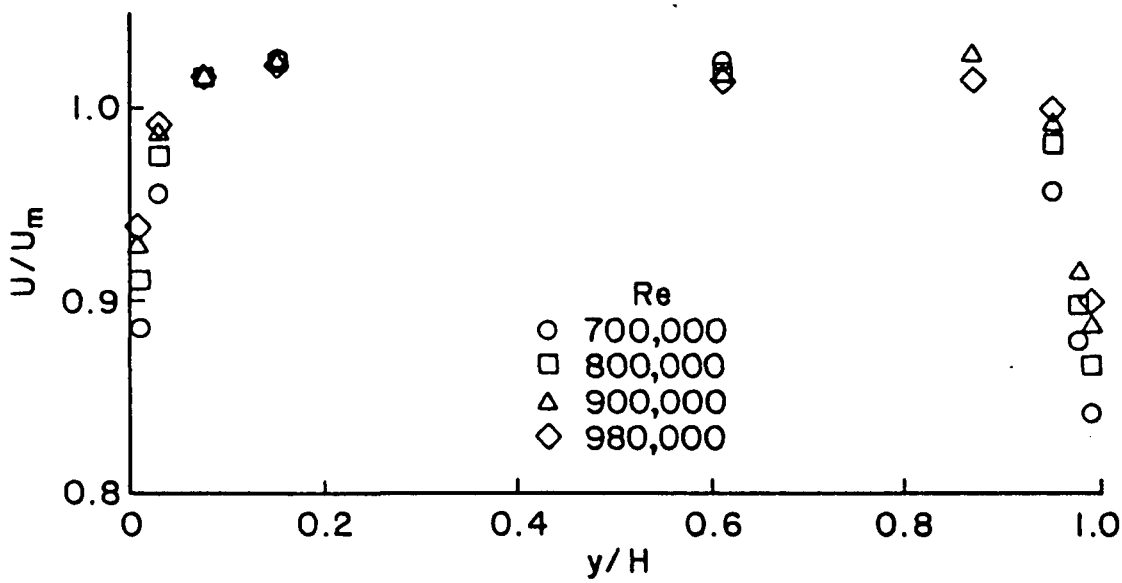

a) Duct Inlet

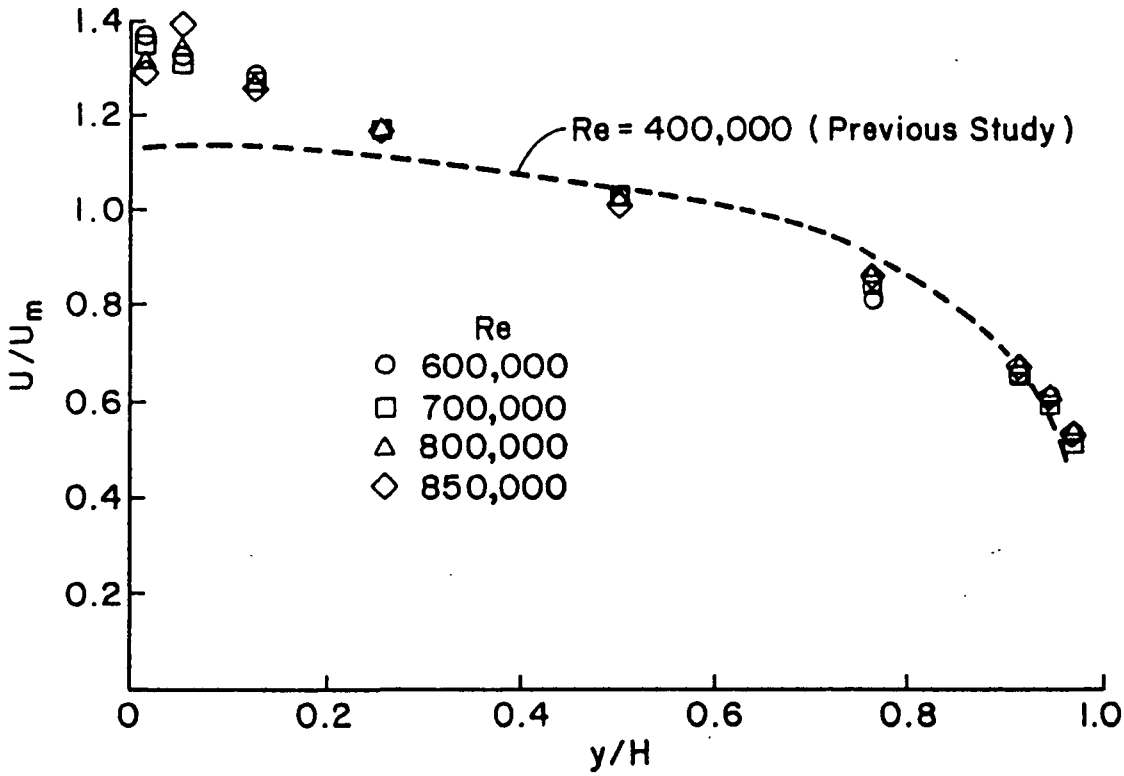

b) Start of the Turn

Figure 3. Mean velocity distributions.

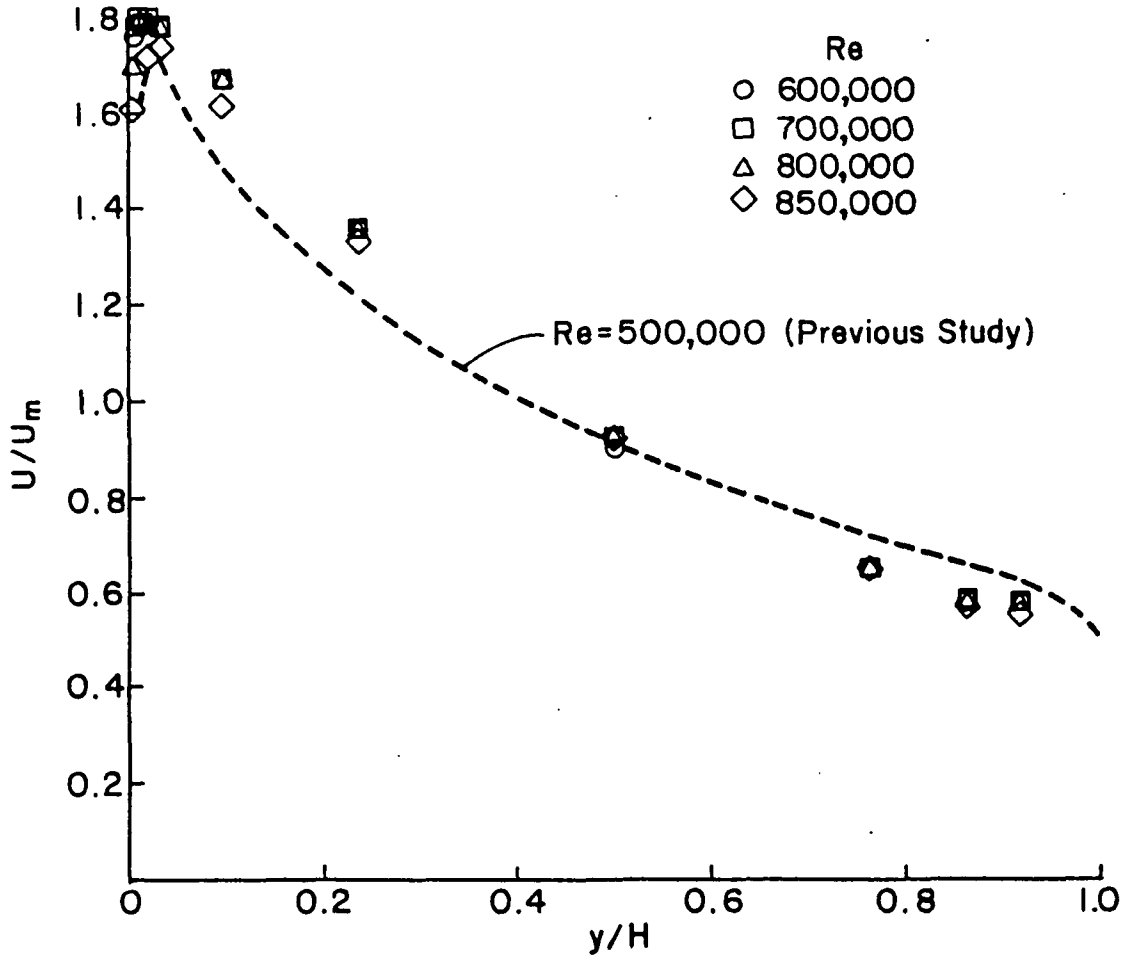

c) 90 degrees Around the Turn

Figure 3. (Cont.) Mean velocity distributions.

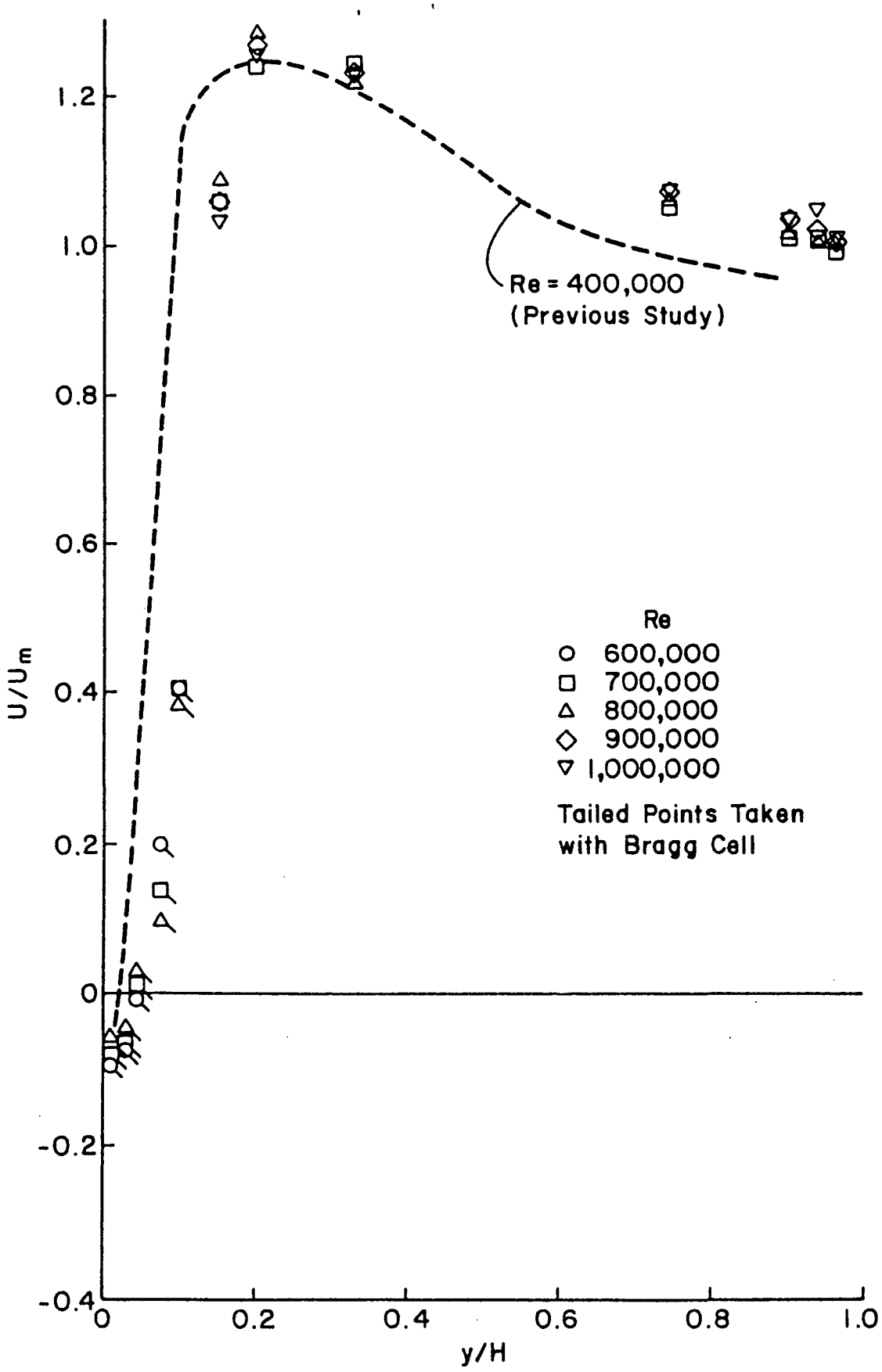

d) Exit of the Turn

Figure 3. (Cont.) Mean velocity distributions.

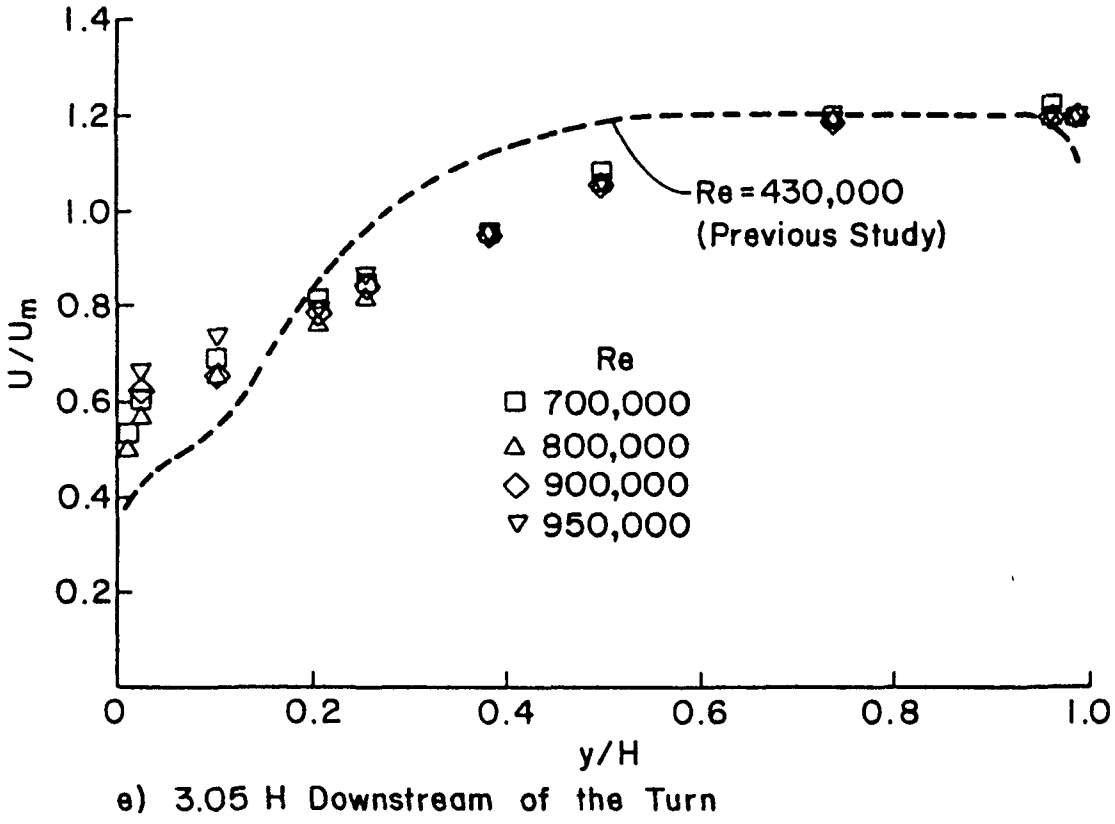

Figure 3. (Concluded) Mean velocity distributions.

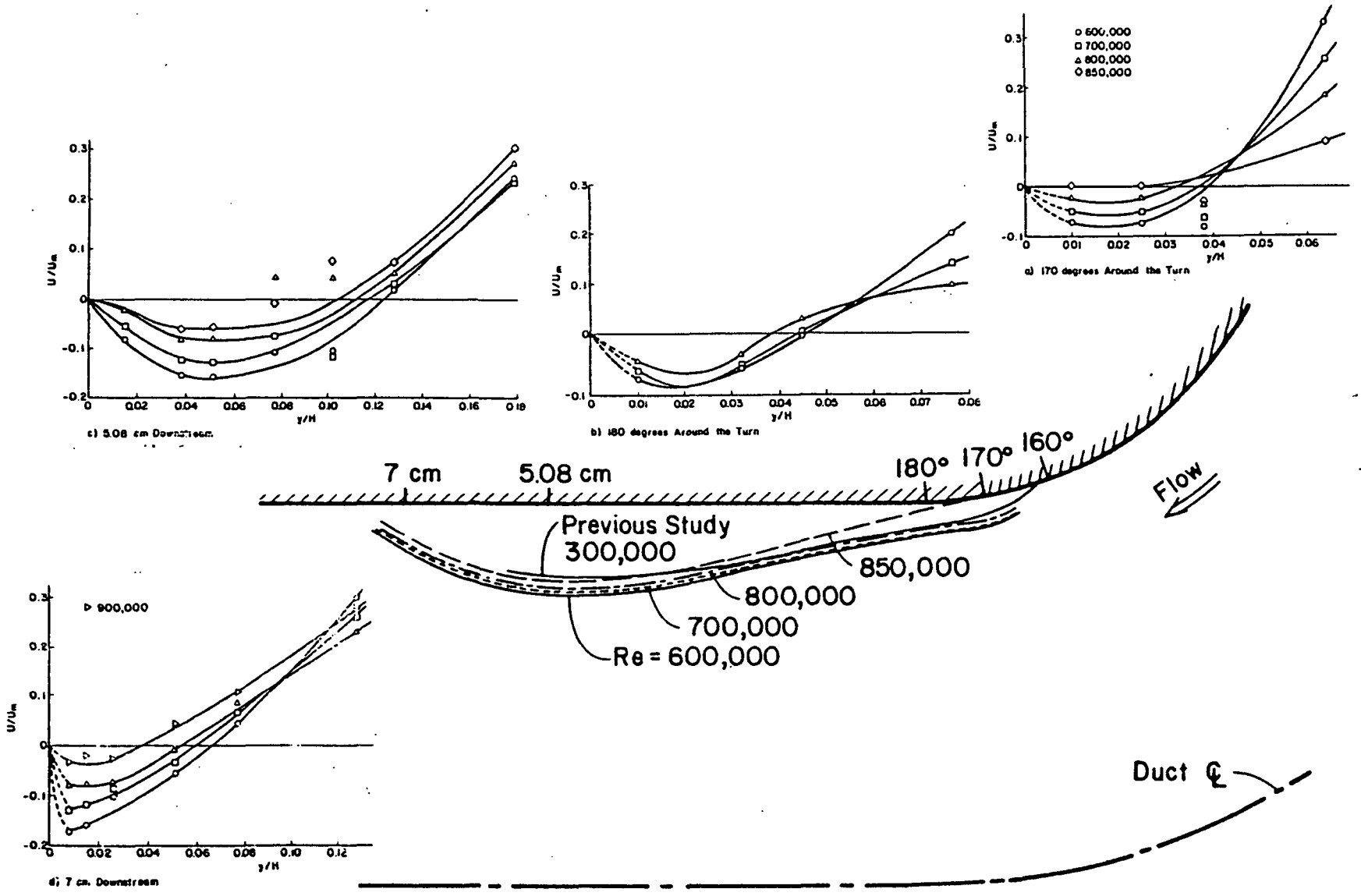

Figure 4. Measurements in the separation bubble region.

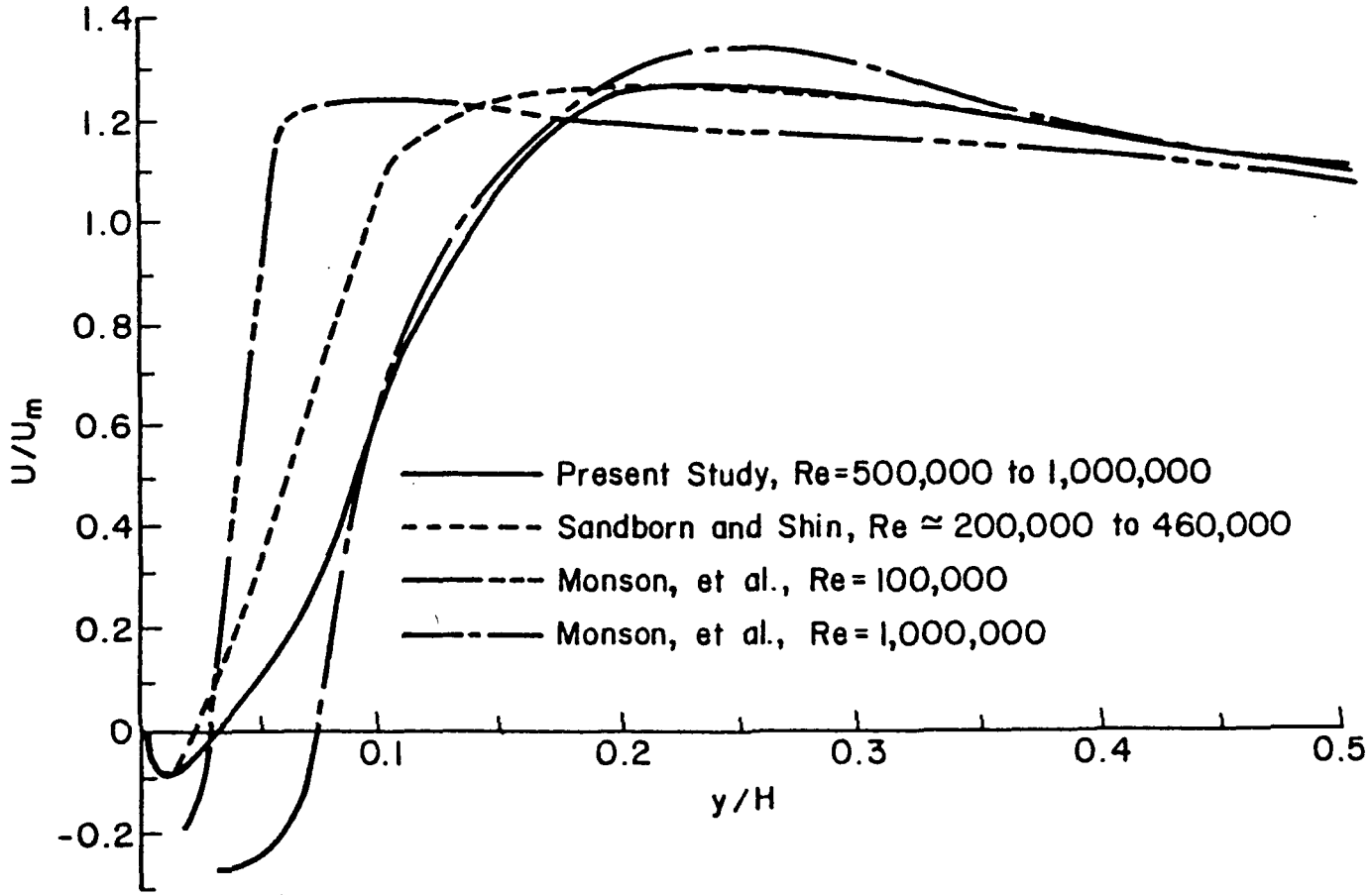

Figure 5. Comparison of the velocity distributions at the turn exit with measurements of Monson, et al (1989).

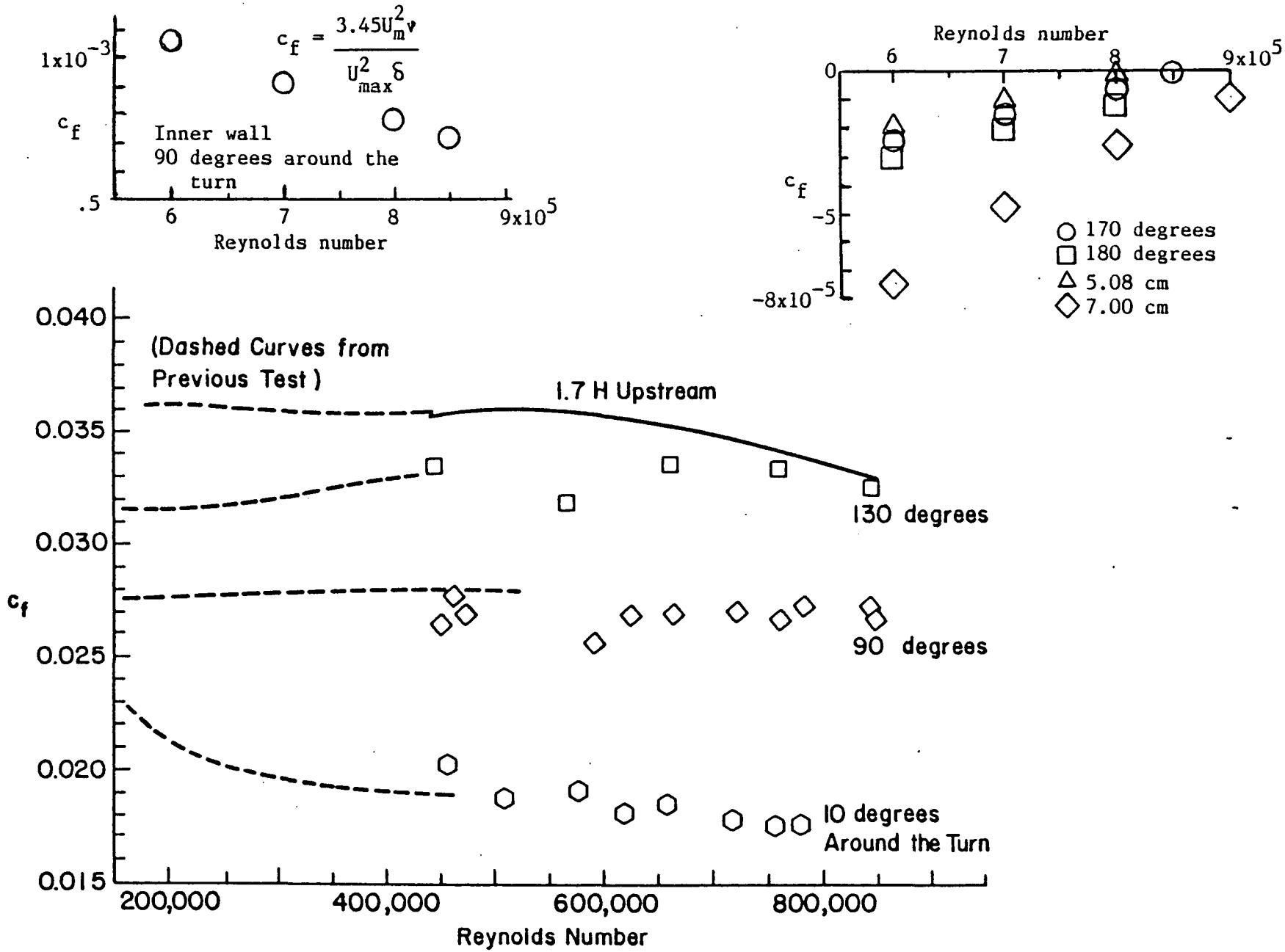

Figure 6. Skin friction coefficient variation with Reynolds number on the outer wall.

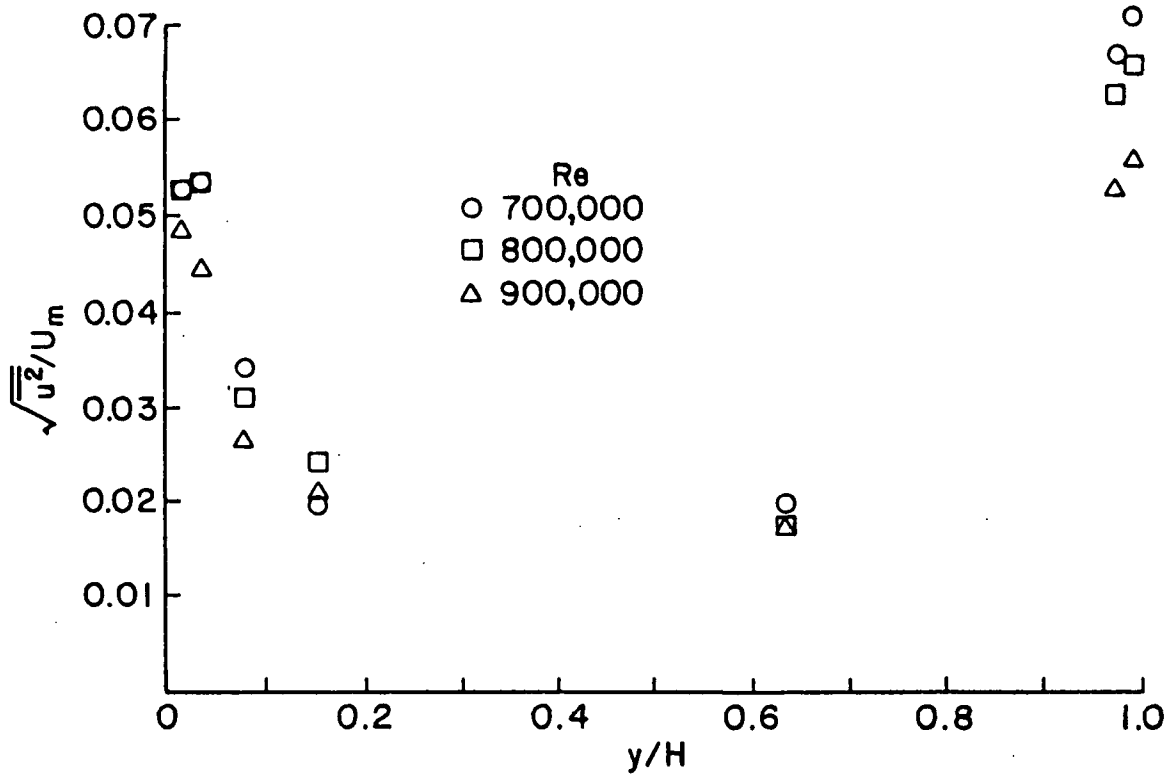

a) Inlet

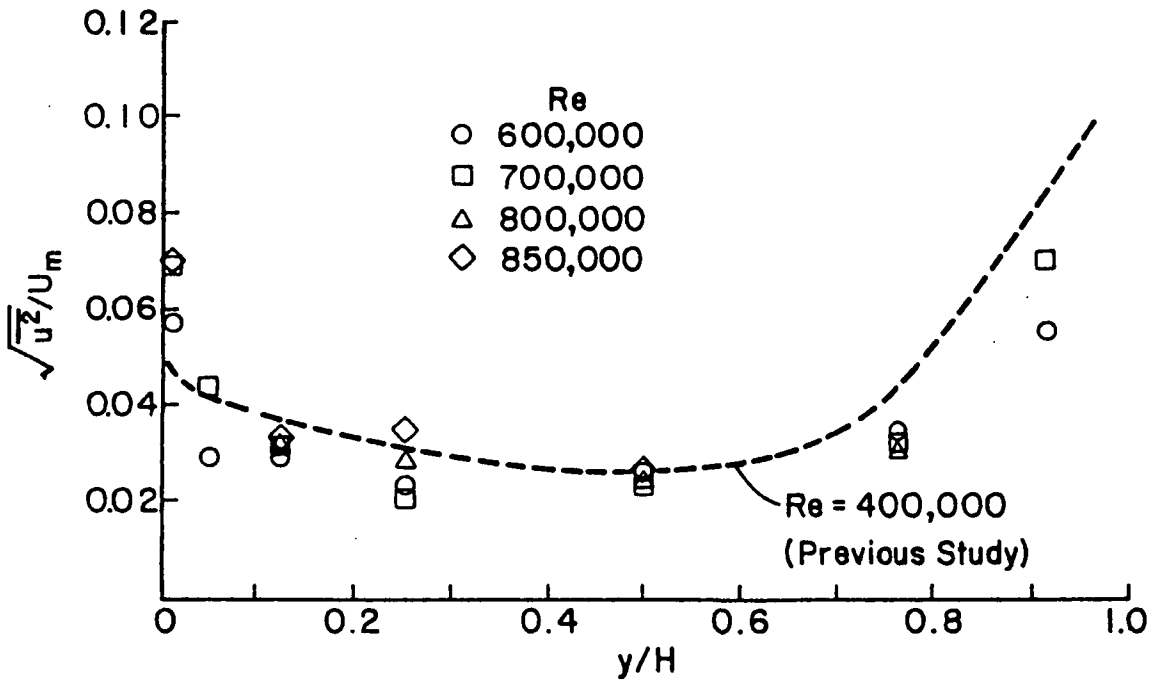

b) Start of the Turn

Figure 7. Tangential turbulent velocity distributions.

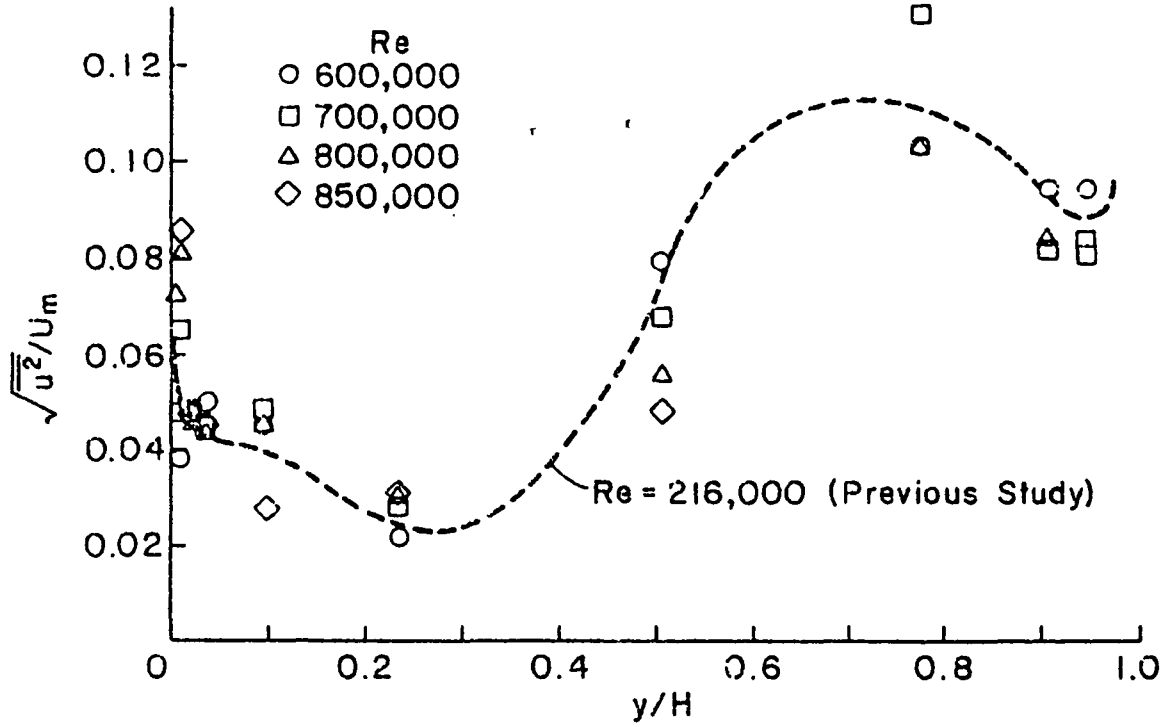

c) 90 degrees Around the Turn

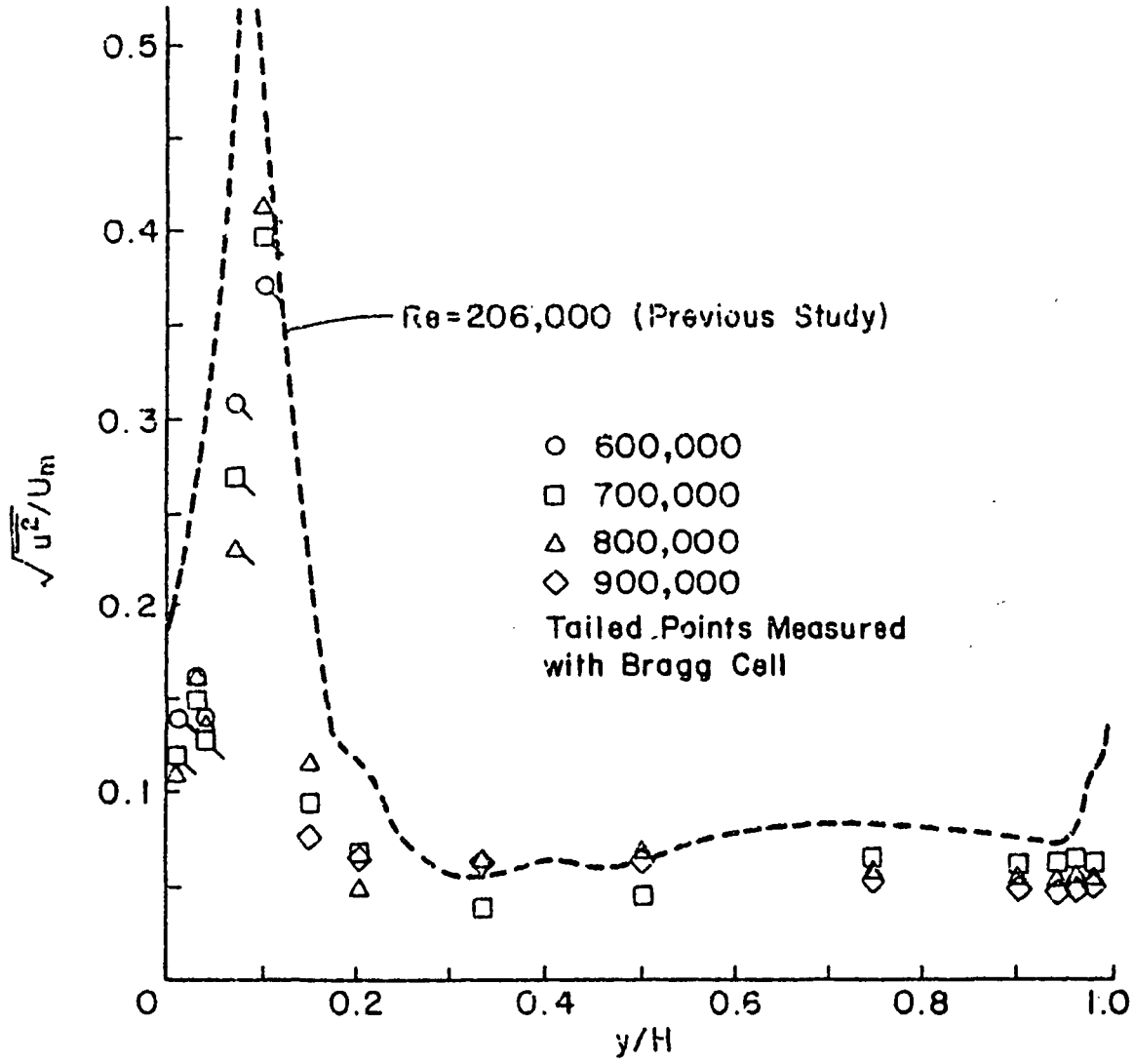

d) Exit of the Turn

Figure 7. (Cont.) Tangential turbulent velocity distributions.

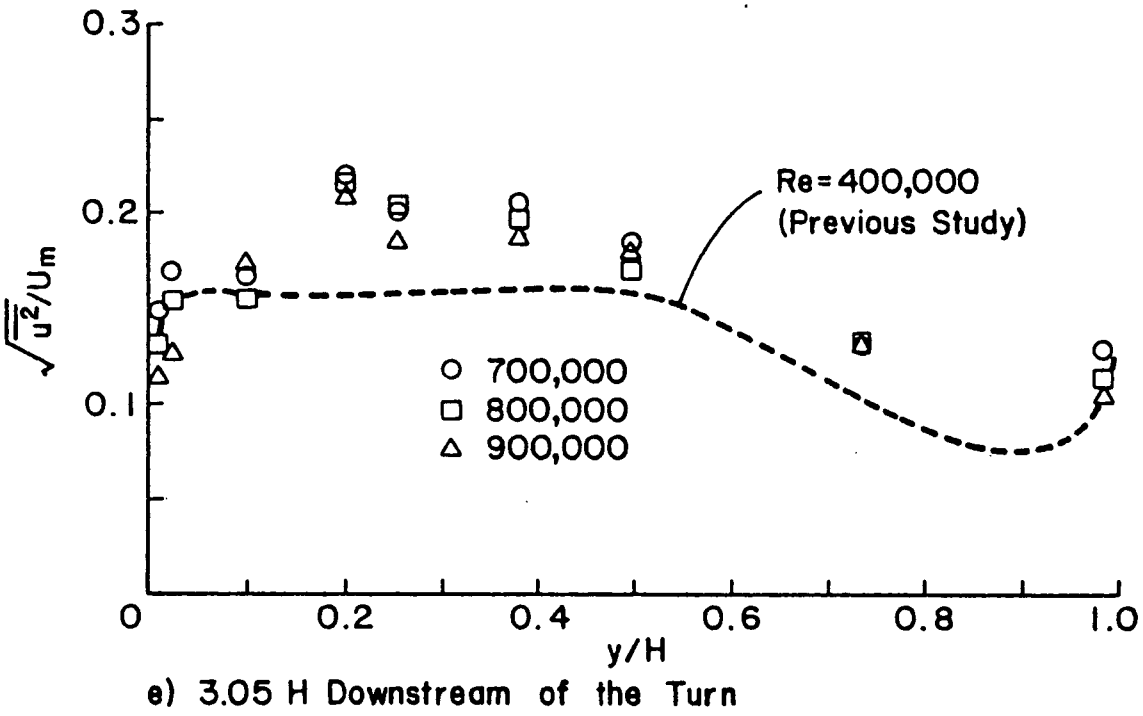

Figure 7. (Concluded) Tangential turbulent velocity distributions.

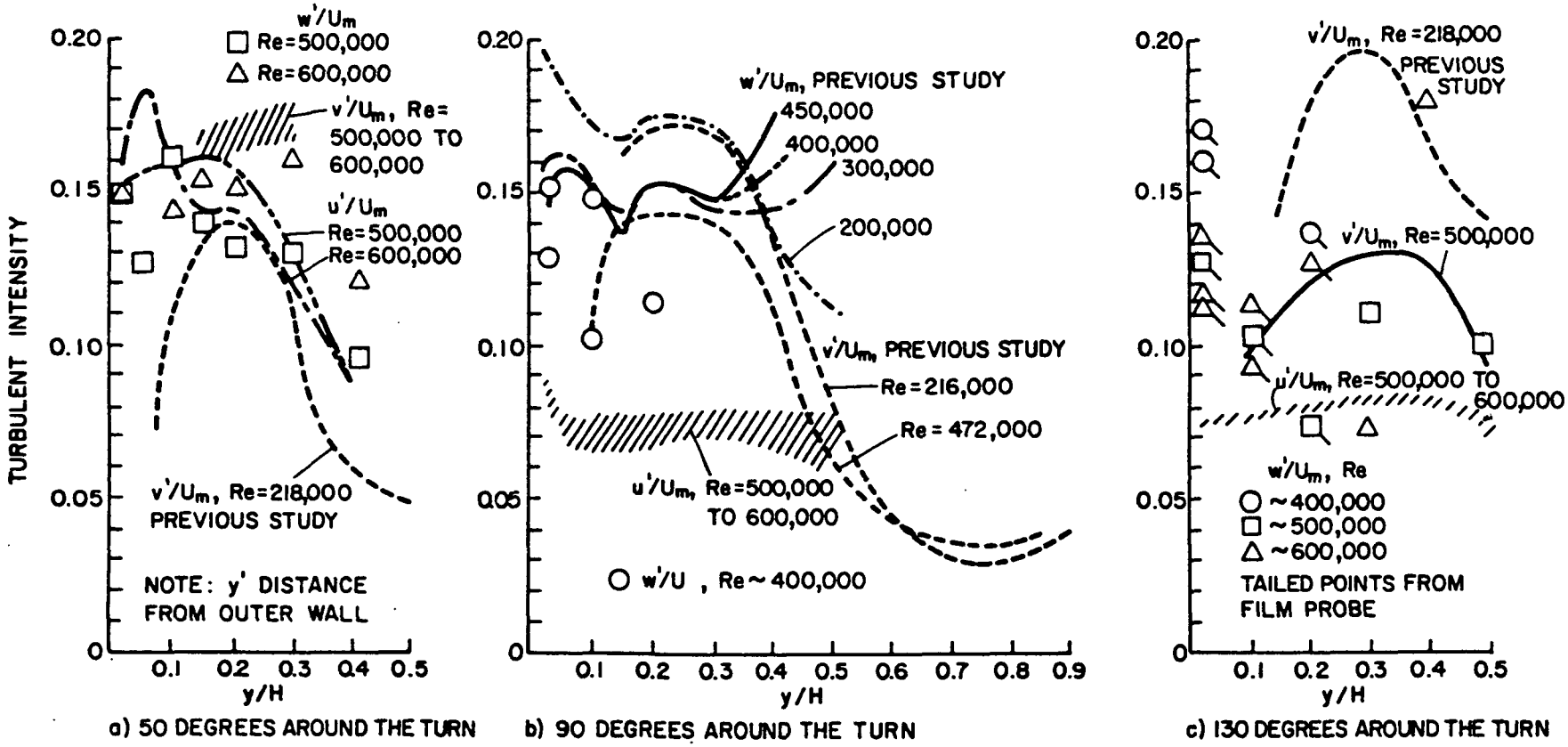

Figure 8. Summary of Turbulent Velocity Fluctuations in the Outer Part of the Turn.

CN22 (0) (2)
TURNER J/PUBLICATION
MARSHALL SPACE FLIGHT CENTER
HUNTSVILLE AL.

DELETIONS OR CHANGES 544-4494
RETURN ADDRESS CN22D 000002444